Biophysical Chemistry 150 (2010) 80–87

Contents lists available at ScienceDirect

Biophysical Chemistry

journal homepage: http://www.elsevier.com/locate/biophyschem

Molecular basis for endotoxin neutralization by amphipathic peptides derived from the α-helical cationic core-region of NK-lysin☆

Klaus Brandenburg [a], Patrick Garidel [b], Satoshi Fukuoka [c], Jörg Howe [a], Michel H.J. Koch [d], Thomas Gutsmann [a], Jörg Andrä [a,*]

[a] Division of Biophysics, Research Center Borstel, Leibniz-Center for Medicine and Biosciences, Borstel, Germany
[b] Physical Chemistry, Martin-Luther University Halle-Wittenberg, Halle/Saale, Germany
[c] National Institute of Advanced Industrial Science and Technology (AIST), Takamatsu, Japan
[d] European Molecular Biology Laboratory, EMBL c/o DESY, Hamburg, Germany

ARTICLE INFO

Article history:
Received 21 December 2009
Received in revised form 21 January 2010
Accepted 21 January 2010
Available online 29 January 2010

Keywords:
Aggregate structure
Antimicrobial peptide
Calorimetry
Endotoxin
Lipopolysaccharide
Small-angle X-ray scattering

ABSTRACT

An analysis of the interaction of the NK-lysin derived peptide NK-2 and of analogs thereof with bacterial lipopolysaccharide (LPS, endotoxin) was performed to determine the most important biophysical parameters for an effective LPS neutralization. We used microcalorimetry, FTIR spectroscopy, Zeta potential measurements, and small-angle X-ray scattering to analyze the peptide:LPS binding enthalpy, the accessible LPS surface charge, the fluidity of the LPS hydrocarbon chains, their phase transition enthalpy change, the aggregate structure of LPS, and how these parameters are modulated by the peptides. We conclude that (i) a high peptide:LPS binding affinity, which is facilitated by electrostatic and hydrophobic interactions and which leads to a positive Zeta potential, (ii) the formation of peptide-enriched domains, which destabilize the lipid packing, demonstrated by a drastic decrease of phase transition enthalpy change of LPS, and (iii) the multilamellarization of the LPS aggregate structure are crucial for an effective endotoxin neutralization by cationic peptides.

1. Introduction

The number of human pathogenic bacteria resistant against common antibiotics is rapidly increasing, whereas at the same time the development of new antibiotics is becoming increasingly time-consuming and expensive. During the last decades new drugs have been based mainly on modifications of existing antibiotics and it is only after a gap of almost 30 years that a really new class of antibiotics like linelozid was discovered and approved for the treatment of bacterial infections. A disadvantage of traditional antibiotics is that these compounds induce the release of lipopolysaccharide (LPS) from the outer membrane of Gram-negative bacteria, one of the most potent activators of the human immune system, which may lead to severe inflammation [1]. Concentrations as small as 10 pg/ml released into the bloodstream activate mononuclear cells (MNC) and macrophages to produce mediators and pro-inflammatory cytokines such as IL6 and tumor necrosis factor (TNF)α [2]. Chemically, LPS is a glycolipid consisting of the lipid A portion, a diglucosamine with up to 7 acyl chains attached through *O*- and *N*-glycosidic linkages, and a sugar chain of variable length (Fig. 1). Generally, a local activation of the immune system may be beneficial for the host, however, a more general systemic activation may lead to sepsis and the septic shock syndrome, which causes at least some hundreds of thousands of deaths/year in Europe only [3]. LPS is therefore also termed endotoxin and lipid A, anchoring the LPS into the membrane, is called the 'endotoxic principle' of LPS. Therapeutic approaches to prevent LPS-induced cell activation and sepsis utilizing TNFα- or LPS-neutralizing antibodies only had limited success [4]. Over the last years antimicrobial peptides (AMPs), now also referred to as host defence peptides, have attracted increasing interest as potent new anti-infectives; [5–8]. AMPs are small, cationic peptides, with an amphipathic secondary structure, which are thought to act by a rapid destruction of the membrane rather than by interaction with specific receptors. This unique mode of action hinders the development of resistances by bacteria and may be the reason that those compounds were conserved in evolution and are nowadays spread among virtually all species as important antimicrobial effector molecules of their innate immune system. Though many groups have investigated natural AMPs and their modifications in terms of antibacterial activities and LPS-neutralizing capacity, the precise mode of action of these substances is

Abbreviations: AMP, antimicrobial peptide; DSC, differential scanning calorimetry; FTIR, Fourier-transform infrared; ITC, isothermal titration calorimetry; LPS, lipopolysaccharide; MNC, mononuclear cells; SAXS, small-angle X-ray scattering; TNFα, tumor necrosis factor α.

☆ Dedicated to Prof. Dr. Alfred Blume on the occasion of his 65th birthday.

* Corresponding author. Division of Biophysics, Research Center Borstel, Leibniz-Center for Medicine and Biosciences, Parkallee 10, D-23845 Borstel, Germany. Tel.: +49 4537 188280; fax: +49 4537 188632.
E-mail address: jandrae@fz-borstel.de (J. Andrä).

0301-4622/$ – see front matter © 2010 Elsevier B.V. All rights reserved.
doi:10.1016/j.bpc.2010.01.009

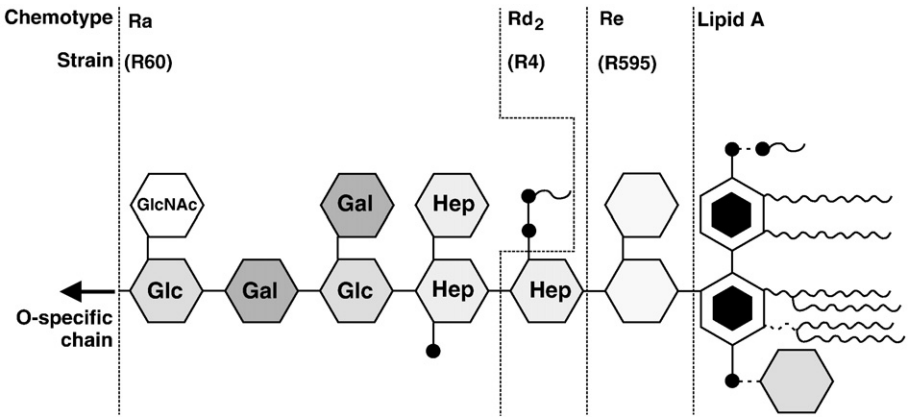

Fig. 1. Schematic chemical structures of different LPS chemotypes. LPS Re, Rd1, and Ra from rough mutants from *Salmonella enterica* Sv Minnesota were used in this study.

still a matter of debate. In particular, very little is known about their molecular basis for their endotoxin neutralization, despite their efficacy in animal models of experimentally-induced sepsis [9–12].

A very promising candidate peptide, termed NK-2, was derived from NK-lysin [13], an all α-helical effector protein from porcine NK- and T-cells with homologs found in human (granulysin) [14], protozoa (amoebapores) [15] and other species [16]. NK-2 is a 27 amino acid residue peptide (Table 1) which represents the cationic core-region (i.e. helices 3 and 4) of NK-lysin [17,18]. The peptide NK-2 adopts an amphipathic α-helical conformation in a membrane-mimetic environment [18,19] and exhibits a broad spectrum activity against Gram-negative, Gram-positive bacteria, and fungi (e.g. against *Escherichia coli*, *Salmonella*, *Staphylococcus aureus* (incl. a methicillin resistant strain), and *Candida albicans*) but it has a low hemolytic activity and cytotoxicity [18,19]. NK-2 most likely acts by disrupting the cytoplasmic membrane and its selectivity may be attributed to differences in the membrane composition of the target cells [20–22]. In addition, the positively charged peptide binds to the negatively charged bacterial lipopolysaccharide with high affinity and neutralizes the endotoxic properties of LPS [23] by preventing the LPS-induced activation of human immune cells and subsequent liberation of pro-inflammatory cytokines such as TNFα. Hence, NK-2 may fulfill a dual role in therapeutics: to effectively kill bacteria, including those resistant against frequently used antibiotics, and simultaneously neutralize the LPS released in the process and prevent sepsis.

In a previous paper we have performed a biophysical analysis of the interaction of NK-2 with LPS [23]. LPS neutralization by NK-2 is accompanied by a compensation of the negative surface potential of LPS and by a reaggregation of the LPS supramolecular structure from a unilamellar/cubic into a multilamellar one. In order to obtain a better understanding of the molecular mechanism of endotoxin neutralization by cationic peptides, we have designed a series of NK-2-derived peptides and correlated their biological activities with biophysical data on the interaction of these peptides with various biomembrane mimetic systems. In a second step, these results might facilitate the optimization of the therapeutic performance of the NK-2 peptide by further sequence variation.

Table 1
Sequence, length (n), net charge (Q), mean hydrophobicity (H), and amphipathicity (μ_H) of NK-2 and derived synthetic peptides. All peptides were synthesized with an amidated C-terminus.

Peptide	Sequence	n	Q	H	$\mu_H(n)$	$\mu_H(7)$
NK-2	KILRGVCKKIMRTFLRRISKDILTGKK	27	+10	−0.27	0.44	0.95
NK27	KILRGVSKKIMRTFLRRISKDILTGKK	27	+10	−0.28	0.43	0.94
NK23b	KILRGVSKKIM RRISKDILTGKK	23	+9	−0.32	0.44	0.88
NK22b	KIL GVSKKIM RRISKDILTGKK	22	+8	−0.22	0.49	0.91
NK19b	KILRGVSKKIM RR ILTGKK	19	+8	−0.32	0.47	0.84
NK15	KILRGVSK R ILTGKK	15	+7	−0.28	0.49	0.74
NK14	KIL GVSK R ILTGKK	14	+6	−0.16	0.36	0.47
NK11	KI SK R ILTGKK	11	+6	−0.37	0.44	0.55
NK10	I SK R ILTGKK	10	+5	−0.32	0.37	0.46

2. Materials and methods

2.1. Peptides

NK-lysin derived peptides were synthesized with an amidated C-terminus by the Fmoc solid-phase peptide synthesis technique on an automatic peptide synthesizer (model 433 A; Applied Biosystems) as described [23]. The net charge (Q) of the peptides was calculated by subtracting the number of aspartic acid residues (the only negatively charged amino acid residues present in the peptides) from all the positive charges (lysine, arginine and the peptide's N-terminus). Since the C-terminus of all peptides used was amidated, it did not bear a negative charge. The mean hydrophobicities (H) and hydrophobic moments (μ_H) of the peptides were calculated as described previously [19] using the consensus scale of hydrophobicity proposed by Eisenberg et al. [24].

2.2. Lipids and reagents

Rough type LPS from various strains of *Salmonella enterica* (serovar Minnesota) were extracted by the phenol/chloroform/petrol ether method from bacteria grown at 37 °C, purified, and lyophilized [25]. LPS of the chemotypes Re (from strain R595), Rd1 (from strain R4), and Ra (from strain R60) was used (see the chemical structures in Fig. 1).

2.3. Preparation of endotoxin aggregates

LPS was solubilized in buffer (see respective method), by vortexing, sonicated in a water bath at 60 °C for 30 min, cooled down to room temperature, and subjected to three or four cycles of heating to 60 °C and cooling down to room temperature. After this procedure, the lipid samples were stored at least 12 h at 4 °C before use.

2.4. Stimulation of human mononuclear cells (MNC) by LPS

Human MNC, isolated from heparinized blood of healthy donors [26], were resuspended in medium (RPMI 1640, 4% human serum) and their number was equilibrated to 5×10^6 cells/ml. For stimulation, 200 µl MNC (1×10^6 cells) were transferred into each well of a 96-well culture plate. LPS Ra from *S. enterica* strain R60 and [peptide]:[LPS] mixtures (10:1 and 20:1 (w/w), which correspond to molar ratios of 7.5:1 and 15:1 for NK-2, and of 3:1 and 6:1 for NK11, respectively) were incubated for 30 min at 37 °C and added to the cultures at 20 µl per well

(final LPS concentrations: 0.3, 1, 3, and 10 ng/ml). The cultures were incubated for 4 h at 37 °C under 5% CO_2. Supernatants were collected after centrifugation of the culture plates for 10 min at 400×*g*, stored overnight at 4 °C and used for the immunological determination of TNFα in a Sandwich ELISA using a monoclonal antibody against TNFα (clone 6b from Intex AG, Switzerland) as described earlier in detail [27].

2.5. Zeta potential measurements

LPS Re samples (0.1 mM) from *S. enterica* strain R595 were dispensed in 10 mM Tris, 2 mM CsCl, pH 7.0, temperature-cycled three times between 20 °C and 60 °C and stored at room temperature. Peptide samples (1–5 mM) were dissolved in the same buffer. The LPS dispersions were then mixed at different ratios with the peptide solution or with pure buffer. The electrophoretic mobility of LPS aggregates was determined in an electric field of 19.2 V/cm with a Zetasizer 4 (Malvern Instruments, Herrenberg, Germany) by laser-Doppler anemometry at a scattering angle of 90° at room temperature. The Zeta potential was then calculated according to the Helmholtz–Smoluchovski equation.

2.6. Isothermal titration calorimetry (ITC)

Microcalorimetric experiments of peptide binding to LPS were performed on a MSC isothermal titration calorimeter (Microcal Inc., Northhampton, MA, USA) at 40 °C as described previously [28]. Briefly, after thorough degassing of the samples, peptides (1–4 mM in 20 mM HEPES, pH 7.0) were titrated to an LPS Ra suspension (0.05 mM in 20 mM HEPES, pH 7.0) of *S. enterica* strain R60. The enthalpy change during each injection was measured by the instrument, the area underneath each injection peak was integrated (Origin, MicroCal, Inc., Northhampton, MA, USA), and plotted against the [peptide]:[LPS] molar ratio. Titration of the pure peptide into HEPES buffer resulted in a negligible endothermic reaction due to dilution, which was subtracted from the plotted curves. The experiments were done at least twice.

2.7. Differential scanning calorimetry (DSC)

DSC measurements were performed with a VP-DSC calorimeter (MicroCal, Inc., Northhampton, MA, USA) at a heating and cooling rate of 0.5 °C min^{-1}. The DSC samples were prepared by dispersing a known amount of LPS Ra from *S. enterica* strain R60 (~3 mg/ml) in 10 mM sodium phosphate buffer, pH 7.4. The samples were hydrated in the liquid-crystalline phase by vortexing. Prior to the measurements the DSC samples were stored for a defined time at 4 °C (see text). The measurements were performed between 10 °C and 80 °C. Up to 20 consecutive heating and cooling scans were performed to check the reproducibility of the DSC experiments of each sample. The accuracy of the DSC experiments was ±0.1 °C for the main phase transition temperatures and ±1 kJ mol^{-1} for the main phase transition enthalpy change. The DSC data were analyzed using the Origin software (MicroCal, Inc., Northhampton, MA, USA). The phase transition enthalpy change was obtained by integrating the area under the heat capacity curve [29].

2.8. Fourier-transform infrared (FTIR) spectroscopy

The infrared spectroscopic measurements were performed on an IFS-55 spectrometer (Bruker, Karlsruhe, Germany). Samples of LPS Ra from *S. enterica* strain R60 were dissolved in 20 mM HEPES buffer, at pH 7.0, and were placed in a CaF_2 cuvette with a 12.5 μm teflon spacer. Temperature-scans were performed automatically between 10 and 70 °C with a heating-rate of 0.6 °C/min. Every 3 °C, 50 interferograms were accumulated, apodized, Fourier transformed, and converted to absorbance spectra. For strong absorption bands, the band parameters (peak position, band width, and intensity) were evaluated from the original spectra, if necessary after subtraction of the strong water bands.

2.9. Small-angle X-ray scattering (SAXS)

X-ray diffraction measurements were made at the European Molecular Biology Laboratory (EMBL) outstation at the Deutsches Elektronen Synchrotron (DESY, Hamburg) using the double-focusing monochromator-mirror camera X33 [30]. Diffraction patterns in the range of scattering vector $0.07 < s < 1\ nm^{-1}$ ($s = 2 \sin\theta/\lambda$, 2θ scattering angle and λ the wavelength = 0.15 nm) were recorded from the LPS Rd1 samples (5 mg/ml) from *S. enterica* strain R4 at different temperatures with exposure times of 2 or 3 min using a data acquisition system with a linear detector with delay line readout [31,32]. The *s*-axis was calibrated with tripalmitin which has a periodicity of 4.06 nm at room temperature. The diffraction patterns were evaluated as described previously [33] by assigning the spacing ratios of the main scattering maxima to defined three-dimensional structures. The lamellar and cubic structures are most relevant here. They are characterized by the following features: (i) Lamellar: The reflections are grouped in equidistant ratios, i.e., 1, 1/2, 1/3, 1/4, etc. of the lamellar repeat distance d_L. (ii) Cubic: The different space groups of these non-lamellar three-dimensional structures differ in the ratio of their spacings. The relation between reciprocal spacing $s_{hkl} = 1/d_{hkl}$ and lattice constant a is $s_{hkl} = [(h^2 + k^2 + l^2)/a]^{1/2}$ (hkl = Miller indices of the corresponding set of plane).

3. Results

3.1. Design of NK-2 variants

The parent protein of NK-2, porcine NK-lysin, is stabilized by three disulfide bridges, among others between cys35 and cys45. To address stability of NK-2, we substituted the remaining, no longer functional, sole cysteine residue (cys45) within its sequence (residues 39–65 corresponding to NK-lysin) by a serine residue (C7S), resulting in the peptide NK27. Furthermore, helical parts of NK-2 were omitted to reduce the peptide length but maintain its amphipathic nature (i.e. the overall hydrophobicity and hydrophobic moment) and the charge pattern of NK-2. Following this strategy, several new peptides ranging from 10 to 27 amino acid residues in length were synthesized (Table 1, see also [19]).

Their biological activity (i.e. LPS-neutralizing capacity with well defined LPS chemotypes) was measured and their interactions with LPS aggregates were investigated in detail by biophysical means. Different LPS chemotypes were used to account for experimental constraints of the various biophysical methods. In particular the peptide/LPS binding reaction and the gel to liquid-crystalline phase transition were studied by calorimetry, the LPS acyl chain fluidity and its aggregate structure with FTIR spectroscopy and SAXS. These are all parameters which have been previously found to be crucial for the modulation of the biological activity of endotoxin [23,34–40].

3.2. Inhibition of the LPS-induced activation of human immune cells

The capacity of the synthetic peptides to inhibit cell activation by rough type LPS Ra was determined with MNC freshly isolated from human blood. Cell activation was monitored by immunological determination of the pro-inflammatory cytokine TNFα in the supernatant of stimulated MNC (Fig. 2). Peptides NK-2 and NK27 were equally active at a [peptide]:[LPS] weight ratio of 20:1 and resulted in an almost complete inhibition of cell activation up to 10 ng/ml LPS Ra. However, at reduced peptide excess ratio ([peptide]:[LPS] = 10:1), NK-2 demonstrated superiority over peptide NK27. The shortened peptide variants exhibited a drastically reduced LPS-neutralization activity with NK19b as the most active derivative. Note that the omission of a

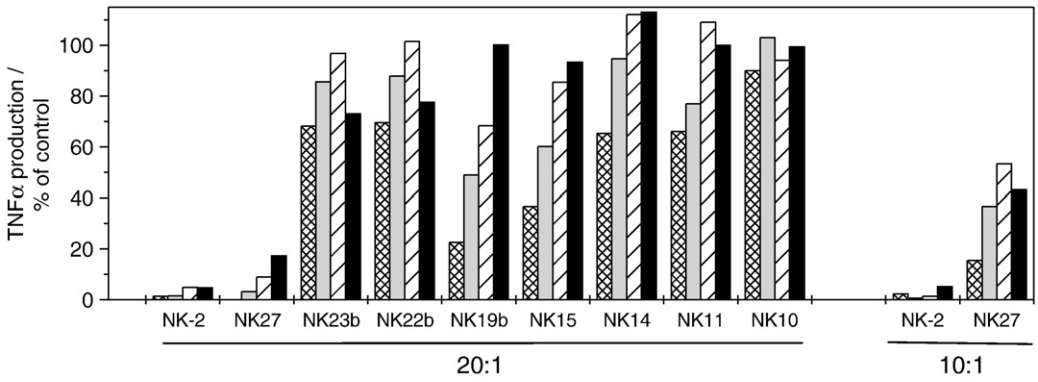

Fig. 2. Peptide-mediated inhibition of the LPS-induced activation of human immune cells. Peptides were mixed with rough type LPS Ra from *S. enterica* strain R60 at two different peptides to LPS ratios (w/w) as indicated. Subsequently, four dilutions of the mixtures were used to stimulate MNC: 0.3 ng/ml LPS Ra (cross-hatched bars), 1 ng/ml (grey bars), 3 ng/ml (hatched bars), and 10 ng/ml (black bars). As a marker of LPS-induced cell activation, the production of the cytokine TNFα was determined by ELISA. Note that a peptide:LPS Ra ratio of 10:1 at the highest LPS Ra concentration used in this assays (10 ng/ml) corresponds to a peptide concentration in cell culture of only 0.1 μg/ml.

single positively charged arginine residue (ΔR4) in peptides NK23b and NK15 leading to peptides NK22b and NK14, respectively, had no effect in case of NK23b/NK22b, however, significantly impaired the capacity of the NK14 peptide to inhibit the LPS-induced cell activation. The shortest peptide NK10 was completely inactive.

3.3. Peptide binding to LPS aggregates

Peptide binding to LPS aggregates was investigated by ITC and by determination of the Zeta potential of the aggregates, which is a measure of the accessible surface charge of aggregates. For ITC, a selection of peptides (NK-2, NK23b, NK19b, NK15, NK11) was titrated subsequently to LPS Ra suspensions at 40 °C and the enthalpy changes were monitored. From the raw data, the dilution enthalpy change was subtracted and the binding heats are shown (Fig. 3). These titrations led to negative enthalpy changes at 40 °C corresponding to exothermic reactions. The values of ΔH directly correlated with the binding strength, with by far the highest values for NK-2 (−34 kJ/mol) and lowest for NK11 (−9 kJ/mol). Similarly, the binding stoichiometry correlated with the activity of the peptides: For NK11 a much higher peptide concentration was needed to reduce the ΔH values, which ideally should end at zero values when the charge compensation is complete. It should be noted that no reasonable curve could be fitted for peptide NK19b. The titration of this peptide to LPS aggregates displayed a biphasic behaviour, probably due to the co-existence of LPS in the gel and liquid-crystalline phase (see also SAXS data below).

The Zeta potential of LPS aggregates was determined from their electrophoretic mobility at room temperature (Fig. 4). All investigated peptides induced a clear decrease of the Zeta potential for LPS Re from around −60 mV in the absence of peptides and to values around 0 mV at a [peptide]:[LPS] molar ratio of 1 and higher for all peptides, except for the parent peptide NK-2. For this peptide, positive Zeta potentials around +20 to +25 mV were observed (Fig. 4) at high peptide concentration, indicating that additional amounts of NK-2 bind to LPS beyond pure charge neutralization.

3.4. Influence of peptides on the LPS phase transition and acyl chain fluidity

The influence of the peptides on the phase properties and fluidity of the LPS acyl chains was monitored by FTIR spectroscopy and DSC. As a general observation, the data indicate that the peptides shift the temperature T_C of the gel (β) to liquid-crystalline (α) phase transition of the LPS acyl chains and reduce the enthalpy change ΔH of this transition (Figs. 5A, B, 6, Table 2). This is accompanied by a loss of cooperativity, evidenced by a broadening of the enthalpy change peak (Fig. 6, Table 2). The FTIR and DSC results reveal different tendencies whereby T_C apparently decreases in the FTIR, but increases in DSC scan. This observation may be due to the formation of peptide-enriched domains. It should be noticed that the IR signal is an average of all methylene stretching vibrations of the sample, independent whether the hydrocarbon chains adopt an all-trans or gauche conformation. Using DSC, however, the transition from one phase to another is observed, e.g. the phase transition from the gel phase to a liquid-crystalline phase. Lipids, which undergo no phase transition, are not detected as a phase transition. Thus, although both methods yield information about changes in phase transition, the combined results allow a much deeper understanding of the interaction mechanism between the lipid and the

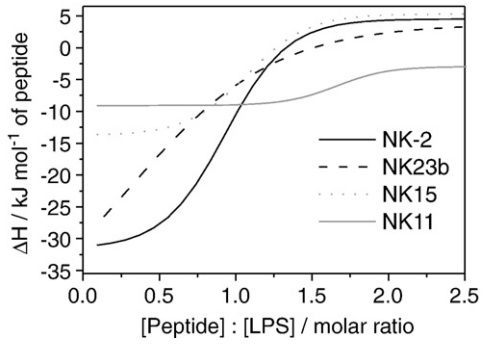

Fig. 3. Enthalpy change of the peptides to LPS binding reaction. Selected peptides were titrated every 5 min to a 0.05 mM LPS suspension (*S. enterica* strain R60) at 40 °C and the resulting enthalpy change was monitored by ITC. The negative enthalpy change indicates an exothermic reaction.

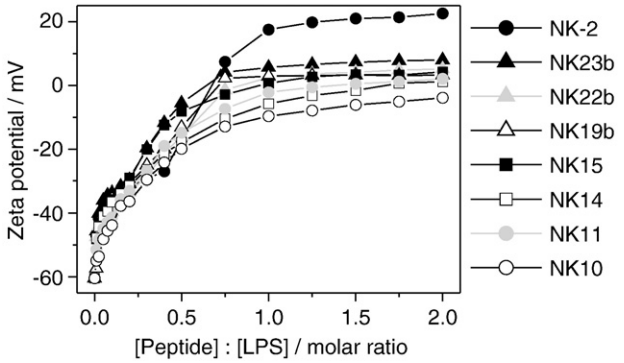

Fig. 4. Zeta potential of peptide:LPS aggregates. The Zeta potential of various [peptide]:[LPS] Re mixtures from *S. enterica* strain R595 was determined from their electrophoretic mobility at room temperature.

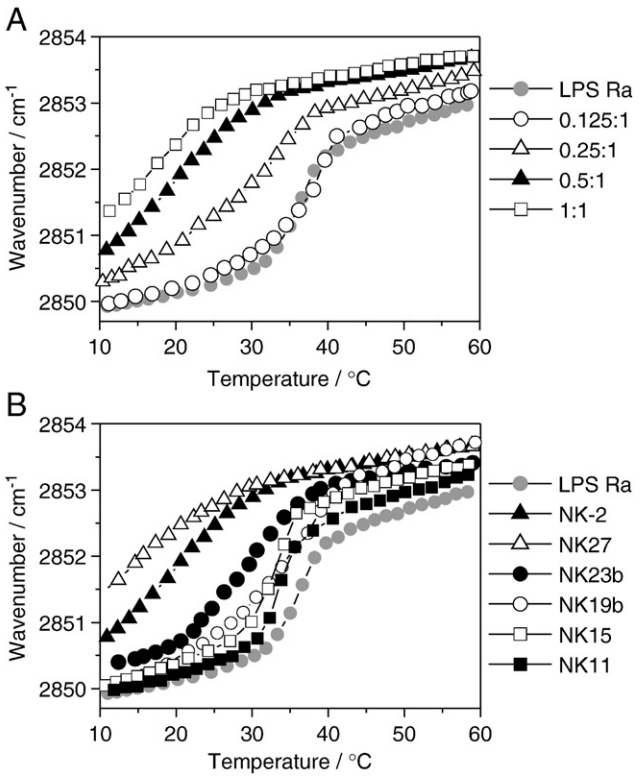

Fig. 5. Influence of peptides on the acyl chain fluidity and phase transition behaviour of LPS. The LPS phase behaviour was monitored over the peak position of the symmetric stretching vibration of the methylene groups of the acyl chains of LPS Ra from *S. enterica* strain R60 in the presence of NK-2 at various [peptide]:[LPS] molar ratios (A) and of derived synthetic peptides at a fixed [peptide]:[LPS] molar ratio of 0.5. In the gel (β) phase of the acyl chains, the peak lies around 2850 cm^{-1}, in the liquid-crystalline (α) phase around 2853 cm^{-1}.

peptide (see discussion below). One must be aware that the strongly acting peptides such as NK-2 cause a drastic broadening of the phase transition in the FTIR measurement which may not be detectable in the DSC scan. Similarly, a change in the heat capacity signal is observed only at high peptide concentrations (Fig. 6) with a drastic decrease of Δ*H*, to which the FTIR experiment may not be sensitive. Moreover, addition of the peptides strongly fluidizes the LPS acyl chains in the gel as well as in the liquid-crystalline phase as can be deduced from the higher wavenumber values (Fig. 5A, B). This fluidization was more pronounced for the more active peptides. Furthermore, at a distinct [peptide]:[LPS] molar ratio (i.e. 0.5:1), there is a clear correlation between T_C and Δ*H*

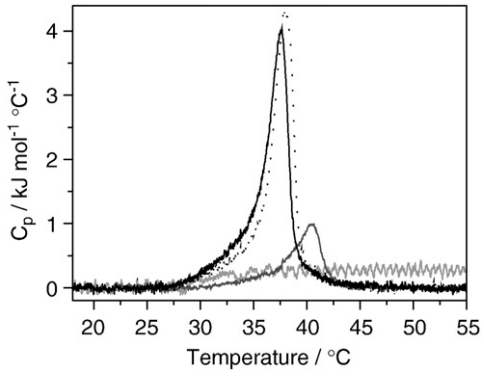

Fig. 6. Influence of peptide on the phase transition enthalpy change of LPS. Phase transition enthalpy changes of LPS Ra (solid black line) from *S. enterica* strain R60 and of [NK-2]:[LPS] mixtures at molar ratios of 0.1:1 (dotted black line), 0.3:1 (grey) and 1:1 (light grey) were determined by DSC. The heat capacity C_p is plotted against temperature.

Table 2
Thermodynamic data for LPS Ra (*S. enterica*) and mixtures thereof with NK-2 derivatives. T_C, phase transition temperature; ΔT_C, difference of T_C of the respective peptide:LPS mixture to T_C of pure LPS; $T_{1/2}$, full width at half maximum of T_C; n.a., not applicable.

	[Peptide]:[LPS] (molar ratio)	T_C (°C)	ΔT_C (°C)	$T_{1/2}$ (°C)	ΔH (kJ mol^{-1})	ΔH (%)
LPS	–	37.7	–	2.3	14.4	100
NK-2	0.05	38.0	+0.3	2.0	15.7	109
	0.1	38.1	+0.4	2.2	14.0	97
	0.2	38.7	+1.0	2.6	11.7	81
	0.3	40.7	+3.0	3.2	3.8	26
	0.4	42.6	+4.9	6.8	3.5	24
	1	n.a.	–	n.a.	0	0
NK27	0.05	38.0	+0.3	2.1	14.8	103
	0.1	38.4	+0.7	2.1	14.8	103
	0.2	40.2	+2.5	3.3	10.4	72
	0.4	42.1	+4.4	8.7	4.3	30
NK19b	0.05	38.2	+0.5	1.9	15.1	105
	0.1	38.1	+0.4	1.9	15.3	106
	0.2	40.2	+2.5	3.9	12.4	86
	0.4	41.8	+4.1	6.6	5.8	40
	1	n.a.	–	n.a.	0	0
NK15	0.05	38.3	+0.6	2.6	12.8	89
	0.1	38.7	+1.0	3.3	13.2	92
	0.2	38.7	+1.0	6.4	13.7	95
	0.4	40.6	+2.9	7.8	9.1	63
	1	n.a.	–	n.a.	0	0
NK11	0.05	38.3	+0.6	2.6	13.8	96
	0.1	38.1	+0.4	3.6	14.9	103
	0.2	38.4	+0.7	4.9	14.7	102
	0.4	39.6	+1.9	6.1	11.3	78
	1	32.7	−5.0	4.2	1.8	13

and the LPS-neutralizing capacity of the peptides (NK-2 > NK27 > NK23b > NK19b > NK15 ≫ NK11). At an equimolar [peptide]:[LPS] ratio, the phase transition vanishes for all tested peptides, except for the biologically inactive NK11 (Fig. 6, Table 2). At this high [peptide]:[LPS] molar ratio values for T_C and Δ*H* could not be determined.

3.5. LPS aggregate structure

For a detailed structural and functional analysis we selected the most interesting representatives among the nine peptides (i.e. a series of four peptides ranging from the most active to the almost inactive) (NK-2, NK23b, NK19b, and NK11). The peptides exhibited a significantly different impact on the aggregate structure of LPS. For pure LPS Rd1, we observed a broad, relatively unstructured diffraction pattern typical for the form factor in the scattering curve (a lipid bilayer) superimposed by peaks which may correspond to a cubic structure (Fig. 7A). Here, the actual type of the aggregate structure cannot be given. It is known, however, that all enterobacterial LPS have a tendency to form cubic structures [41]. In the presence of peptides NK-2, NK23b, and NK19b this structure is changed into a pure multilamellar one, characterized by strong peaks with a periodicity between 7.06 and 7.97 nm and higher order reflections at 1, 1/2, and 1/3 of the periodicity (Fig. 7A, B). The double peaks for NK23b and NK19b indicate that two periodicities can be observed, which most likely reflect the co-existence of LPS in the gel and in the liquid-crystalline phase. This might be due to one less and one strongly disturbed LPS multilayer, or domain formation, because the main spacings correspond to those found when pure LPS Rd1 adopts a multilamellar structure (e.g. in the presence of Mg^{2+} [41]). NK11 however, had no significant impact on the pattern of the LPS supramolecular aggregate, which was nearly the same as without peptide. NK-2 was more closely analyzed at a [peptide]:[LPS] ratio of 0.1:1 molar (Fig. 7B). At 20 °C, there are two multilamellar stacking periodicities with $d_{l1} = 7.97$ nm with higher orders around 4.00 nm and 2.67 nm, and $d_{l2} = 5.81$ nm with a second order at 2.92 nm. The second periodicity indicates the formation of peptide-enriched

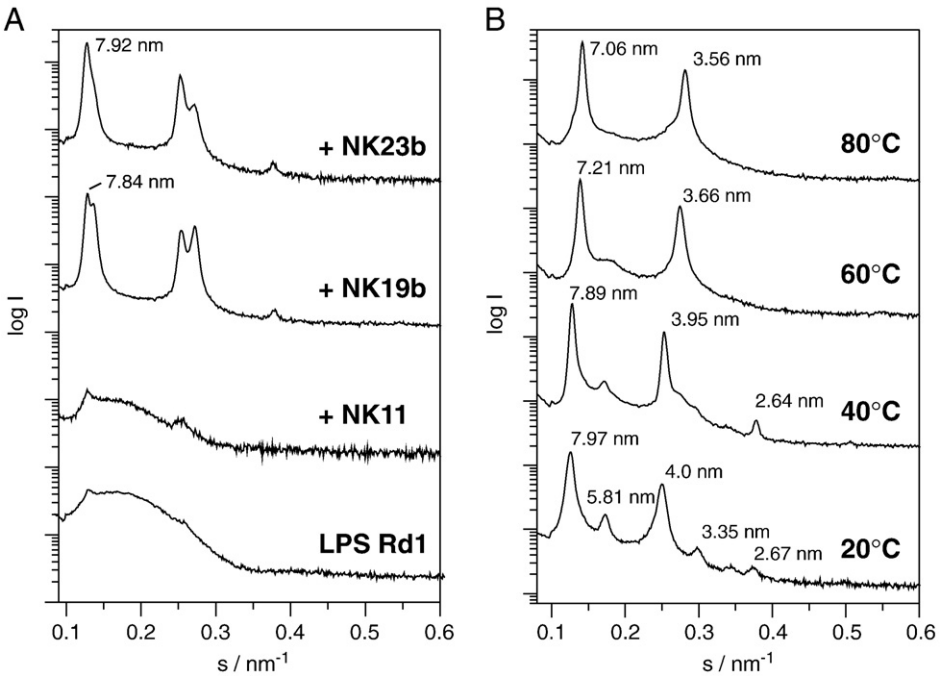

Fig. 7. Influence of NK-2 derived peptides on the supramolecular structure of LPS. LPS Rd1 aggregates from *S. enterica* strain R4 with and without peptides were analyzed by SAXS. The logarithm of the scattering intensity ($\log I_{(s)}$) is plotted against the scattering vector $s\ (=1/d, d =$ spacings of the reflections) for (A) pure LPS and [peptide]:[LPS] mixtures at a molar ratio of 0.1:1 at 40 °C, and (B) [NK-2]:[LPS] mixture at a molar ratio of 0.1:1 at indicated temperatures. Note the occurrence of a second lamellar periodicity indicating the formation of peptide-enriched domains, which is not observed in the presence of the less active peptides NK19b and NK23b.

domains which are not formed in the presence of the other peptides. The diffraction peak at 3.35 nm is not directly assignable. It maybe, however, that this reflection corresponds to the second order reflection of another multilamellar structure, where the first order reflection is not visible on the right slope of the main peak centered at 7.97 nm. At higher temperatures, the patterns convert progressively into that characteristic of a structure with a single main periodicity. Additionally, the decrease of the spacings from 7.89 nm to 7.21 nm between 40 °C and 60 °C is characteristic for the transition from the gel into the liquid-crystalline phase (see respective paragraph).

4. Discussion

We have designed and synthesized antimicrobial peptides on the basis of the cationic core of NK-lysin to find out how changes in the amino acid sequence of the well-described 'mother' peptide NK-2 [18,19,23] influence the ability to neutralize bacterial endotoxin and also to determine the most important physicochemical parameters for an effective binding of endotoxin. The inhibition experiments of the LPS-induced cytokine production in human MNC clearly indicate that the longer peptides have the highest activity (Fig. 2). In the absence of the peptides, LPS is present as aggregates with a cubic inverted structure which has been shown to represent the bioactive unit of all enterobacterial endotoxins [42]. Upon addition of peptides, this aggregate structure converts into multilamellar stacks (Fig. 7A, B), which has previously been shown to be the necessary condition for endotoxin detoxification [35]. Our data clearly indicate that the extent of multilamellarization is directly connected with the ability of the peptides to inhibit cytokine production (Figs. 2 and 7). Reflections in equidistant ratios are sharper and more pronounced for peptides with a higher ability to suppress the LPS-induced TNFα secretion. Moreover, the occurrence of a second periodicity in the presence of NK-2 indicates the formation of peptide-enriched domains which have not been observed for the less active peptides. Parallel to this change of the aggregate structure, the hydrocarbon chains of LPS are fluidized (Fig. 5A and B) as found earlier for the 'gold standard' lipopeptide polymyxin B [43,44]. The extent of fluidization at a fixed LPS:peptide ratio apparently also directly correlates with the inhibition activity. Concomitantly, the enthalpy change ΔH of the gel to liquid-crystalline phase transition is reduced (Fig. 6, Table 2). The combined results from FTIR and DSC allow a deeper understanding of the interaction mechanism between the lipid and the peptide. In FTIR a shift of the phase transition to lower temperature accompanied by a strong broadening of the phase transition is observed, which indicates that the gel phase is destabilized in the presence of peptides. The derived information from FTIR is an average information of the systems, i.e. an average signal of all hydrocarbon chains. DSC shows that the phase transition is shifted to higher temperature, and that the phase transition enthalpy change is decreased. A decrease in the phase transition enthalpy change is a clear indication that the peptide interacts with the lipid such that the lipid phase is completely transformed (abolished) and no phase transition is observed. Phase segregation and domain formation is a reason for this. At low peptide concentrations at least two phases co-exist: (i) One lipid population interacts strongly with the peptides accompanied with a drastic reduction of ΔH. This population is not visible in DSC scans, however, dominates the FTIR signal. (ii) The other lipid population, interacts weakly or not with the peptides, which led to the observed shift of T_C in the DSC scans. Only the contributions from the lipids undergoing a phase transition are detected in DSC by a DSC peak. Due to the fact that the phase transition enthalpy change is decreased, the formation of a second peptide-enriched lipid phase undergoing no phase transition in the investigated temperature range is likely. This peptide-enriched lipid phase may also fit in the concept of trapped lipid domains, which has been developed to describe co-existing lipid phases in lipid monolayers [45]. The reason for the shift to higher temperature of the observed phase could be due to hydration changes of these lipids [46,47].

The most effective peptides have the strongest enthalpy change ΔH (not to mix with the ΔH of the phase transition) for binding to LPS, and reach binding saturation much earlier than less effective peptides (Fig. 3). It has been shown that the negative binding enthalpy change, an exotherm, results from the Coulomb interaction between the

positive charges of the peptides and the negative charges of LPS, which is the dominant process in the liquid-crystalline phase of LPS (the data in Fig. 3 were obtained at 40 °C). This process of LPS neutralization is connected with a compensation of the surface charges of LPS. Again, the most active peptides lead to the most positive signals (i.e. NK-2 followed by NK23b) (Fig. 4). Interestingly, effective LPS neutralization apparently is connected with an overcompensation of the Zeta potential of LPS aggregates upon peptide binding. This phenomenon has been described before for two distinct sets of peptides of different origin and structure namely T-shaped lactoferricin [38], and cyclic peptides derived from the *Limulus* anti-LPS factor (LALF) [37]. Furthermore, we showed that the LPS-neutralizing capacity of the peptide as well as the antibacterial activity is dependent on the LPS sugar chain length, which are likely to shield against cationic drugs [23,38,48].

The changes in the LPS aggregate structure, connected with more fluid hydrocarbon chains and a decrease in surface charge density due to the peptide binding, strongly influence the interaction with mammalian binding proteins, the first of which have been described being LBP and CD14 [49,50]. Binding of LPS to these proteins competes with its binding to the peptides, and LPS retains its activity only if the bound peptides are displaced (i.e. the binding constant for LBP:LPS must be higher than for peptide:LPS). This is apparently the case for the peptides with short amino acid chain length, which are displaced from the peptide:LPS complex. The LPS:LBP complex is then transported to the immune cells and intercalates into the membrane [51]. In contrast, for the peptides with longer amino acid chain length, the degree of multilamellarization and with that the high peptide:LPS binding constant, inhibits the binding of LBP to the LPS epitopes.

Structural prerequisites for peptides to inactivate LPS were found to be a sufficient high number of basic (positively charged) amino acid residues such as lysine (K) and arginine (R), which have to match the distance of the negatively charged lipid A headgroup phosphates to guarantee the Coulomb/electrostatic interactions [52], as well as the presence of some hydrophobic amino acid residues such as leucine (L), isoleucine (I) and phenylalanine (F) for the partial intercalation of the peptide into the lipid A moiety in LPS [42]. Whereas the short peptides such as NK10 and NK11 might have a sufficiently high number of positive charges, the number of hydrophobic amino acid residues is obviously too small to bind effectively into the hydrocarbon chains of LPS. Short peptides may be efficient against Gram-negative bacteria, but not against isolated LPS [53,54]. This should be seen in the light of the fact that in the bacterial membranes LPS is present as a lipid monolayer, whereas in isolated form it packs into a cubic aggregate. Therefore, the conditions for optimally acting anti-microbially or anti-endotoxically may differ considerably, as also found for other AMPs [44,55].

In conclusion, we suggest the following biophysical parameters as most important for an effective endotoxin neutralization: (i) high peptide:LPS binding affinity facilitated by electrostatic and hydrophobic interactions leading to a positive Zeta potential, (ii) formation of peptide-enriched domains, which destabilize the lipid packing, demonstrated by a drastic decrease of phase transition enthalpy change, and (iii) rearrangement of the LPS supramolecular structure to a multilamellar stack. These parameters should be considered in any rational approach to develop improved peptides for an anti-sepsis therapy.

Acknowledgements

The authors are indebted to the Deutsche Forschungsgemeinschaft DFG (SFB617, project A17 'Molecular mechanisms of epithelial defence') and the German ministry for Education and Research BMBF ('Therapy of infectious diseases', project 01GU0824) for financial support. J.A. was a recipient of a short-term postdoctoral fellowship of the Japan Society for the Promotion of Science (JSPS). Moreover, part of this work was supported by JSPS Japan–Germany Research Cooperative Program, Grant-in-Aid for Scientific Research (KAKENHI 21550168), and JST Research for Promoting Technological Seeds.

References

[1] E.T. Rietschel, T. Kirikae, F.U. Schade, U. Mamat, G. Schmidt, H. Loppnow, A.J. Ulmer, U. Zahringer, U. Seydel, F. Di Padova, et al., Bacterial endotoxin: molecular relationships of structure to activity and function, FASEB J. 8 (1994) 217–225.
[2] H. Loppnow, H.-D. Flad, E.T. Rietschel, H. Brade, The active principle of bacterial lipopolysaccharides (endotoxins) for cytokine induction, in: G. Schlag, H. Redl (Eds.), Pathophysiology of Shock, Sepsis, and Organ Failure, Springer Verlag, Heidelberg, 1993, pp. 405–416.
[3] A. Legras, B. Giraudeau, A.P. Jonville-Bera, C. Camus, B. Francois, I. Runge, A. Kouatchet, A. Veinstein, J. Tayoro, D. Villers, E. Autret-Leca, A multicentre case–control study of nonsteroidal anti-inflammatory drugs as a risk factor for severe sepsis and septic shock, Crit. Care 13 (2009) R43.
[4] R. Sundaresan, J.N. Sheagreen, Current understanding and treatment of sepsis, Infect. Med. 12 (1995) 261–268.
[5] R. Jerala, M. Porro, Endotoxin neutralizing peptides, Curr. Top. Med. Chem. 4 (2004) 1173–1184.
[6] M. Hirata, Y. Shimomura, M. Yoshida, S.C. Wright, J.W. Larrick, Endotoxin-binding synthetic peptides with endotoxin-neutralizing, antibacterial and anticoagulant activities, Prog. Clin. Biol. Res. 388 (1994) 147–159.
[7] R.E. Hancock, H.G. Sahl, Antimicrobial and host-defense peptides as new anti-infective therapeutic strategies, Nat. Biotechnol. 24 (2006) 1551–1557.
[8] M. Zasloff, Antimicrobial peptides of multicellular organisms, Nature 415 (2002) 389–395.
[9] O. Cirioni, A. Giacometti, R. Ghiselli, F. Mocchegiani, A. Fineo, F. Orlando, M.S. Del Prete, M. Rocchi, V. Saba, G. Scalise, Single-dose intraperitoneal magainins improve survival in a gram-negative-pathogen septic shock rat model, Antimicrob. Agents Chemother. 46 (2002) 101–104.
[10] A. Giacometti, O. Cerioni, R. Ghiselli, F. Orlando, W. Kamysz, M. Rocchi, G. D´Amato, F. Mocchegiani, C. Silvestri, J. Lukasiak, V. Saba, G. Scalise, Effects of pexiganan alone and in combination with betalactams in experimental endotoxic shock, Peptides 26 (2005) 207–216.
[11] A. Giacometti, O. Cirioni, R. Ghiselli, F. Mocchegiani, M.S. Del Prete, C. Viticchi, W. Kamysz, E. Lempicka, V. Saba, G. Scalise, Potential therapeutic role of cationic peptides in three experimental models of septic shock, Antimicrob. Agents Chemother. 46 (2002) 2132–2136.
[12] A. Giacometti, O. Cirioni, R. Ghiselli, C. Viticchi, F. Mocchegiani, A. Riva, V. Saba, G. Scalise, Effect of mono-dose intraperitoneal cecropins in experimental septic shock, Crit. Care Med. 29 (2001) 1666–1669.
[13] M. Andersson, H. Gunne, B. Agerberth, A. Boman, T. Bergman, R. Sillard, H. Jörnvall, V. Mutt, B. Olsson, H. Wigzell, A. Dagerlind, H.G. Boman, G.H. Gudmundsson, NK-lysin, a novel effector peptide of cytotoxic T and NK cells. Structure and cDNA cloning of the porcine form, induction by interleukin 2, antibacterial and antitumour activity, EMBO J. 14 (1995) 1615–1625.
[14] S.V. Peña, A.M. Krensky, Granulysin, a new human cytolytic granule-associated protein with possible involvement in cell-mediated cytotoxicity, Semin. Immunol. 9 (1997) 117–125.
[15] M. Leippe, J. Andrä, R. Nickel, E. Tannich, H.J. Müller-Eberhard, Amoebapores, a family of membranolytic peptides from cytoplasmic granules of *Entamoeba histolytica*: isolation, primary structure, and pore formation in bacterial cytoplasmic membranes, Mol. Microbiol. 14 (1994) 895–904.
[16] J.J. Endsley, J.L. Furrer, M.A. Endsley, M.A. McIntosh, A.C. Maue, W.R. Waters, D.R. Lee, D.M. Estes, Characterization of bovine homologues of granulysin and NK-lysin, J. Immunol. 173 (2004) 2607–2614.
[17] E. Liepinsh, M. Andersson, J.-M. Ruysschaert, G. Otting, Saposin fold revealed by the NMR structure of NK-lysin, Nat. Struct. Biol. 4 (1997) 793–795.
[18] J. Andrä, M. Leippe, Candidacidal activity of shortened synthetic analogs of amoebapores and NK-lysin, Med. Microbiol. Immunol. 188 (1999) 117–124.
[19] J. Andrä, D. Monreal, G. Martinez de Tejada, C. Olak, G. Brezesinski, S. Sanchez Gomez, T. Goldmann, R. Bartels, K. Brandenburg, I. Moriyon, Rationale for the design of shortened derivatives of the NK-lysin derived antimicrobial peptide NK-2 with improved activity against Gram-negative pathogens, J. Biol. Chem. 282 (2007) 14719–14728.
[20] H. Schröder-Borm, R. Willumeit, K. Brandenburg, J. Andrä, Molecular basis for membrane selectivity of NK-2, a potent peptide antibiotic derived from NK-lysin, Biochim. Biophys. Acta 1612 (2003) 164–171.
[21] H. Schröder-Borm, R. Bakalova, J. Andrä, The NK-lysin derived peptide NK-2 preferentially kills cancer cells with increased surface levels of negatively charged phosphatidylserine, FEBS Lett. 579 (2005) 6128–6134.
[22] C. Olak, A. Muenter, J. Andrä, G. Brezesinski, Interfacial properties and structural analysis of the antimicrobial peptide NK-2, J. Pept. Sci. 14 (2008) 510–517.
[23] J. Andrä, M.H.J. Koch, R. Bartels, K. Brandenburg, Biophysical characterization of the endotoxin inactivation by NK-2, an antimicrobial peptide derived from mammalian NK-Lysin, Antimicrob. Agents Chemother. 48 (2004) 1593–1599.
[24] D. Eisenberg, E. Schwarz, M. Komaroy, R. Wall, Analysis of membrane and surface protein sequences with the hydrophobic moment plot, J. Mol. Biol. 179 (1984) 125–142.
[25] C. Galanos, O. Lüderitz, O. Westphal, A new method for the extraction of R lipopolysaccharides, Eur. J. Biochem. 9 (1969) 245–249.
[26] K. Brandenburg, G. Jürgens, J. Andrä, B. Lindner, M.H. Koch, A. Blume, P. Garidel, Biophysical characterization of the interaction of high-density lipoprotein (HDL) with endotoxins, Eur. J. Biochem. 269 (2002) 5972–5981.

[27] G. Jürgens, M. Müller, P. Garidel, M.H. Koch, H. Nakakubo, A. Blume, K. Brandenburg, Investigation into the interaction of recombinant human serum albumin with Re-lipopolysaccharide and lipid A, J. Endotoxin Res. 8 (2002) 115–126.
[28] K. Brandenburg, A. David, J. Howe, M.H.J. Koch, J. Andrä, P. Garidel, Temperature dependence of the binding of endotoxins to the polycationic peptides polymyxin B and its nonapeptide, Biophys. J. 88 (2005) 1845–1858.
[29] C. Johann, P. Garidel, L. Mennicke, A. Blume, New approaches to the simulation of heat-capacity curves and phase diagrams of pseudobinary phospholipid mixtures, Biophys. J. 71 (1996) 3215–3228.
[30] M.H.J. Koch, J. Bordas, X-ray diffraction and scattering on disordered systems using synchroton radiation, Nucl. Instr. Methods 208 (1983) 461–469.
[31] A. Gabriel, Position-sensitive X-ray detector, Rev. Sci. Instrum. 48 (1977) 1303–1305.
[32] W. Shang, B. Robrahn, F. Golding, M.H.J. Koch, Nucl. Instrum. Methods A 530 (2004) 513–520.
[33] K. Brandenburg, W. Richter, M.H.J. Koch, H.W. Meyer, U. Seydel, Characterization of the nonlamellar cubic and H_{II} structures of lipid A from *Salmonella enterica* serovar Minnesota by X-ray diffraction and freeze-fracture electron microscopy, Chem. Phys. Lipids 91 (1998) 53–69.
[34] J. Andrä, P. Garidel, A. Majerle, R. Jerala, R. Ridge, E. Paus, T. Novitsky, M.H.J. Koch, K. Brandenburg, Biophysical characterization of the interaction of *Limulus polyphemus* endotoxin neutralizing protein (ENP) with lipopolysaccharide, Eur. J. Biochem. 271 (2004) 2037–2046.
[35] J. Andrä, T. Gutsmann, P. Garidel, K. Brandenburg, Mechanisms of endotoxin neutralization by synthetic cationic compounds, J. Endotoxin Res. 12 (2006) 261–277.
[36] J. Andrä, J. Howe, P. Garidel, M. Rössle, W. Richter, G.M.d. Tejada, I. Moriyon, R. Bartels, T. Gutsmann, K. Brandenburg, Mechanism of interaction of optimized Limulus-derived cyclic peptides with endotoxins. Thermodynamical and biophysical analysis, Biochem. J. 406 (2007) 297–307.
[37] J. Andrä, M. Lamata, G. Martinez de Tejada, R. Bartels, M.H.J. Koch, K. Brandenburg, Cyclic antimicrobial peptides based on *Limulus* anti-LPS factor for neutralization of lipopolysaccharide, Biochem. Pharmacol. 68 (2004) 1297–1307.
[38] J. Andrä, K. Lohner, S.E. Blondelle, R. Jerala, I. Moriyón, M.H.J. Koch, P. Garidel, K. Brandenburg, Enhancement of endotoxin neutralization by coupling of a C12-alkyl chain to a lactoferricin-derived peptide, Biochem. J. 385 (2005) 135–143.
[39] X. Chen, J. Howe, J. Andrä, M. Rössle, W. Richter, A.P. Galvão da Silva, A.M. Krensky, C. Clayberger, K. Brandenburg, Biophysical analysis of the mechanisms of interaction of granulysin-derived peptides with enterobacterial endotoxins, Biochim. Biophys. Acta 1768 (2007) 2421–2431.
[40] S. Fukuoka, J. Howe, J. Andrä, T. Gutsmann, M. Rössle, K. Brandenburg, Physicochemical and biophysical study of the interaction of hexa- and heptaacyl lipid A from *Erwinia carotovera* with magainin 2-derived antimicrobial peptides, Biochim. Biophys. Acta 1778 (2008) 2051–2057.
[41] U. Seydel, M.H. Koch, K. Brandenburg, Structural polymorphisms of rough mutant lipopolysaccharides Rd to Ra from *Salmonella* minnesota, J. Struct. Biol. 110 (1993) 232–243.
[42] K. Brandenburg, J. Andrä, M. Müller, M.H.J. Koch, P. Garidel, Physicochemical properties of bacterial glycopolymers, Carbohydr. Res. 338 (2003) 2477–2489.
[43] K. Brandenburg, I. Moriyón, M.D. Arraiza, G. Lewark-Yvetot, M.H.J. Koch, U. Seydel, Biophysical investigations into the interaction of lipopolysaccharide with polymyxins, Thermochim. Acta 382 (2002) 189–198.
[44] P. Garidel, K. Brandenburg, Antiinfect, Agents Med. Chem. 8 (2009) 367–385.
[45] H.M. McConnell, P.A. Rice, D.J. Benvegnu, Brownian motion of lipid domains in monolayers, J. Phys. Chem. 94 (1990) 8965–8968.
[46] P. Garidel, A. Blume, The interaction of alkaline earth cations with the negatively charged phospholipid 1, 2-dimyristoyl-sn-glycero-3-phosphoglycerol: a differential scanning and isothermal titration calorimetric study, Langmuir 15 (1999) 5526–5534.
[47] P. Garidel, A. Blume, W. Hubner, A Fourier transform infrared spectroscopic study of the interaction of alkaline earth cations with the negatively charged phospholipid 1, 2-dimyristoyl-sn-glycero-3-phosphoglycerol, Biochim. Biophys. Acta 1466 (2000) 245–259.
[48] R.R. Schumann, S.R. Leong, G.W. Flaggs, P.W. Gray, S.D. Wright, J.C. Mathison, P.S. Tobias, R.J. Ulevitch, Structure and function of lipopolysaccharide binding protein, Science 249 (1990) 1429–1431.
[49] J. Mathison, E. Wolfson, S. Steinemann, P. Tobias, R. Ulevitch, Lipopolysaccharide (LPS) recognition in macrophages. Participation of LPS-binding protein and CD14 in LPS-induced adaptation in rabbit peritoneal exudate macrophages, J. Clin. Invest. 92 (1993) 2053–2059.
[50] P.S. Tobias, K. Soldau, J.A. Gegner, D. Mintz, R.J. Ulevitch, Lipopolysaccharide binding protein-mediated complexation of lipopolysaccharide with soluble CD14, J. Biol. Chem. 270 (1995) 10482–10488.
[51] T. Gutsmann, A.B. Schromm, M.H.J. Koch, S. Kusumoto, K. Fukase, M. Oikawa, U. Seydel, K. Brandenburg, Lipopolysaccharide-binding protein-mediated interaction of lipid A from different origin with phospholipid membranes, Phys. Chem. Chem. Phys. 2 (2000) 4521–4528.
[52] B.T. Japelj, P. Pristovsek, A. Majerle, R. Jerala, Structural origin of endotoxin neutralization and antimicrobial activity of a lactoferrin-based peptide, J. Biol. Chem. 280 (2005) 16955–16961.
[53] K.H. Park, Y.H. Nan, Y. Park, J.I. Kim, I.S. Park, K.S. Hahm, S.Y. Shin, Cell specificity, anti-inflammatory activity, and plausible bactericidal mechanism of designed Trp-rich model antimicrobial peptides, Biochim. Biophys. Acta 1788 (2009) 1193–1203.
[54] K.H. Park, Y. Park, I.S. Park, K.S. Hahm, S.Y. Shin, Bacterial selectivity and plausible mode of antibacterial action of designed Pro-rich short model antimicrobial peptides, J. Pept. Sci. 14 (2008) 876–882.
[55] Y. Rosenfeld, H.G. Sahl, Y. Shai, Parameters involved in antimicrobial and endotoxin detoxification activities of antimicrobial peptides, Biochemistry 47 (2008) 6468–6478.